Open Access

Journal of Energy and Power Technology

LIDSEN Publishing Inc.

Research Article

Study and Characterization of a Spherical Solar Collector. I. Efficiency and Thermal Losses Coefficient

Carlos Armenta-Déu *

Renewable Energy Group, Faculty of Physics, Complutense University of Madrid, 28040 Madrid, Spain; E-Mail: cardeu@fis.ucm.es

* **Correspondence:** Carlos Armenta-Déu; E-Mail: cardeu@fis.ucm.es

Academic Editor: Mariano Alarcón

Special Issue: Solar Thermal Energy

Journal of Energy and Power Technology
2023, volume 5, issue 3
doi:10.21926/jept.2303022

Received: April 21, 2023
Accepted: June 27, 2023
Published: July 04, 2023

Abstract

This paper studies and characterizes a solar collector with spherical geometry to produce hot water for sanitary and domestic applications and other facilities. The new geometry enlarges the solar collector surface and allows full sun tracking during the day without needing a solar tracking system. Although this geometry has been in use for some time, its market penetration is low due to the lack of perfect knowledge of solar collector behavior and the benefits compared with conventional solar collectors. The studies carried out in the lab for small domestic application has shown that this new geometry has better efficiency than flat plate collectors because its particular structure maintains water temperature inside the hot water tank for longer, which allows better production and longer use. The carried-out tests have shown an increase of up to 38% in the collector's efficiency at high-range operation and 13% at the low range. This increase is enlarged to 40% and 15% when dealing with the compact system (collector-storage tank). Global losses coefficient is also lower, around 50%, than for a flat plate solar collector of an equivalent cross-section.

© 2023 by the author. This is an open access article distributed under the conditions of the Creative Commons by Attribution License, which permits unrestricted use, distribution, and reproduction in any medium or format, provided the original work is correctly cited.

Keywords
Solar thermal collector; spherical geometry; efficiency improvement; global thermal losses coefficient

1. Introduction

Flat plate solar collectors are commonly used for hot water production, around 55°C, for domestic uses and other applications. These devices receive lower energy due to the angle of the solar radiation striking the absorber surface. The amount of this energy reduction can be computed through the incidence angle modifier (IAM) [1], achieving up to more than 35% for high latitudes and horizontal surfaces [2]. This reduction is much lower when dealing with lower latitude and tilted surfaces, typically between 5% and 15% [3]. Although the energy losses are lower if the surface is correctly tilted and oriented and placed in locations closer to the equator, the yearly average value of energy losses remains high. We avoid this by using tracking systems [4-6], but using these devices requires a more complex design, provokes the need for power to move the system, and increases the cost of maintenance, which makes the tracking systems useless for small and low-temperature applications such as domestic.

A possible solution to avoid using tracking systems and reducing the IAM is the design of new geometry, which permits the interception of solar radiation throughout the entire day within a minimum angle. The spherical solar collector geometry has been the basic design for this study [7]. The spherical shape allows interception of solar radiation at the same average angle at any time of the solar day length; it does not require a change of the tilt to intercept solar radiation at an acceptable value of IAM when solar altitude is changing [8]. It is true that a flat plate solar collector properly tilted and oriented receives more energy than the sphere but requires a single or two-axis tracking system that reduces the efficiency of the flat plate collector. The final cost of the energy produced is much higher. Therefore, we think that a spherical shape can improve the collection of solar energy, so we have made a detailed study of the performance of this geometry for hot water applications.

An alternative application of spherical solar collectors is air heating since the only change is the heat carrier fluid. In this context, previous studies are of interest for understanding the performance of a new geometry within the field of Solar Air Heaters (SAH) [9-11].

Among the many papers dealing with spherical solar collectors, we find scientific papers devoted to studying the characteristics of the cylindrical receiver [12], evaluating thermal performance [7], or analyzing the ability of sun tracking [13]. Other papers focus on the received solar radiation [14] or the thermal performance in heating water [15]. It looks like the characterization and analysis of the performance of spherical solar collectors are duly covered; however,

This paper tries to contribute to a better understanding of the improvements of spherical solar collectors related to flat-plate ones by evaluating thermal energy efficiency and global thermal losses coefficient in a wide range of operations.

2. Theoretical Background

The following expression rules the energy provided by flat plate solar collector:

$$\dot{Q} = A_c F_R [I - U_L(T_i - T_a)] \tag{1}$$

Where the transfer coefficient F_R is given by:

$$F_R = \left(\dot{m}C_p/A_c U_L\right)\left[1 - \exp\left(-A_c U_L F'/\dot{m}C_p\right)\right] \tag{2}$$

And factor F' is obtained from:

$$F' = \frac{{}^1/_{U_L}}{W\left[\frac{1}{U_L[D + (W - D)F]} + \frac{1}{C_b} + \frac{1}{\pi D_i h_{fi}}\right]} \tag{3}$$

Being:

$$F = \frac{\tanh[m(W - D)/2]}{m(W - D)/2} \tag{4}$$

Expression (1) is by much the most important equation to control the solar collector performance, as it relates the performance of the collector with the operational conditions, the collector characteristics, and the environmental conditions, and it gives the net energy gain as a function of the water inlet temperature. For positive energy gain, it requires:

$$I - U_L(T_i - T_a) > 0 \; or \; T_i > T_a - I/U_L \tag{5}$$

Defining the equivalent temperature, as usual, we have:

$$T_{eq} < 1/U_L \tag{6}$$

The equivalent temperature controls the operational range in which the solar collector produces energy with efficiency above zero. This condition is, however, limited by the minimum temperature required by the application served by the solar collector. According to that, we may define the critical solar radiation level as:

$$I_c = U_L(T_i - T_a) \tag{7}$$

This level defines the zero value for the utilizability function [16], given by:

$$\varphi(I_c) = \frac{\left({}^1/_n\right)\sum_{i=1}^{n}\int_{t_{c-}}^{t_{c+}}(I - I_c)dt}{\left({}^1/_n\right)\sum_{i=1}^{n}\int_{t_{c-}}^{t_{c+}} I dt} \tag{8}$$

From equation (7), we observe that the threshold value of the solar radiation, I_c, depends on the operational conditions, T_i, and the environmental conditions, T_a. It also depends on the solar

characteristics through the thermal losses coefficient, U_L. In a single collector, provided the operational and environmental conditions are constant, the lower U_L is the lower threshold required. However, considering the whole system, including the storage tank, the thermal losses coefficient must be calculated for the collector-tank tandem, which differs from the solar collector coefficient. In many cases, despite the isolation of the tank, the combined value is much higher than the solar collector value alone. Therefore, the global losses are determined by [17]:

$$\dot{Q}_L = U_{L_c}(T_i - T_a) + U_{L_t}(T_t - T_a) \tag{9}$$

If we accept that the solar collector inlet temperature is the same as the average temperature of the tank, we have:

$$\dot{Q}_L = \left(U_{L_c} + U_{L_t}\right)(T_t - T_a) \tag{10}$$

We can see energy losses are higher because the thermal losses coefficient has increased. Because the global losses depend on the tank temperature, the higher the temperature, the greater the thermal losses. Because the thermal losses are mainly produced by radiation, a way to reduce the losses is either by reducing the tank temperature, which limits the number of applications, or the outside temperature, at which the system, collector, and tank radiate energy. If the storage tank is inserted inside the collector structure, so the cover would completely cover the tank, the "outside" temperature "seen" by the tank would be that of the collector, which is even higher, thus reducing to zero the tank losses.

A simple mathematical analysis indicates that the ratio of thermal losses is given by [18]:

$$r_{Q_L} = \frac{1}{1 + \frac{\varepsilon}{\varepsilon'}\frac{S}{S'}\frac{F}{F'}\frac{T_p^4 - T_e^4}{T_{cv}^4 - T_e^4}} \tag{11}$$

Assuming the shape factor to be equal for the tank and collector, and considering the surfaces also equivalents, and because the emissivity of the plate and tank cover are almost identical, the equation (11) converts into:

$$r_{Q_L} = \frac{1}{1 + \frac{T_p^4 - T_e^4}{T_{cv}^4 - T_e^4}} = \frac{T_{cv}^4 - T_e^4}{T_{cv}^4 + T_p^4 - 2T_e^4} \tag{12}$$

If $T_{cv} \approx T_p$, then $r_{Q_L} = 1/2$, which means the new structure reduces the thermal losses by half.

2.1 Solar Collector Efficiency

To determine the solar collector efficiency, we use the same expression as for the flat plate collectors, it is said [19]:

$$\eta_i = Q_u/A_c I = (F_R/I)\left[I\overline{(\tau\alpha)} - U_L(T_i - T_a)\right] \tag{13}$$

The average value (τα) is replaced by the product (τα) due to the perpendicular incidence of solar radiation considered in the spherical collector case [20].

Taking into account the gain balance, which uses the following equation:

$$Q_u = \dot{m}C_p(T_s - T_i) \tag{14}$$

Equation (13) converts into:

$$\eta_i = \left(\dot{m}C_p(T_s - T_i)/A_c I\right) = a[(T_s - T_i)/I] \tag{15}$$

This expression has been used in the study to compute the collector's efficiency as a function of the inlet and outlet temperature.

3. Description of the System

The prototype is a commercial [21] spherical collector of 1.05 m. in diameter, with an effective interception surface of 4.02 m2 (Figure 1), whose selectivity is equal to 19. A transparent plastic cover of high transmissivity (t > 0.95) covers the surface. The spherical surface absorbs direct and diffuse solar radiation from both hemispheres and reflected radiation from the ground. An internal chamber attached to the inner part of the absorber collects the heat from solar radiation, whose upper portion connects to the heat charger placed inside the heating tank. The fluid is a mixture of water and glycol with a boiling point above 115°C and a freezing point below -15°C. An electric pump of 40 W circulates the fluid flow at the primary circuit between the heating tank and the collector. Hot water exits the tank through a rubber duct with a loss coefficient of 0.02°C/m. The heating tank locates at the interior of the collector's structure, so it is protected from the environment by the envelope of the solar collector (see Figure 2).

Figure 1 View of the prototype.

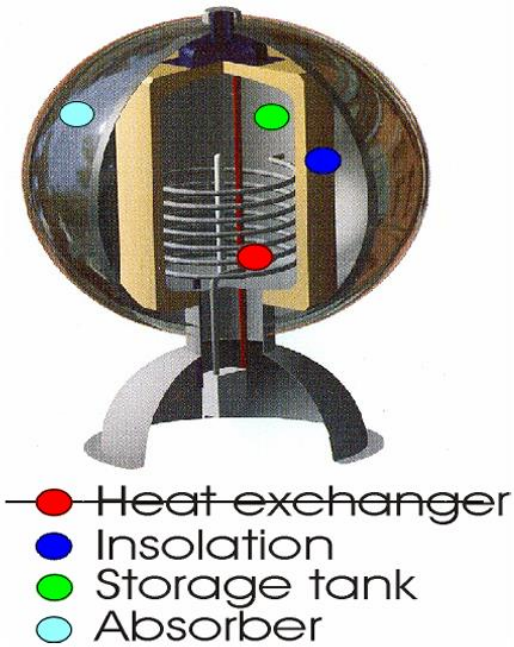

Figure 2 Cutting view of the prototype.

Pt-104 sensors connected to a data logger control the temperature. An SKYE-TORN pyranometer measures horizontal solar radiation. The values are corrected for the appropriate angle using the expression:

$$I = I_{ON} \cdot \cos\theta_Z \tag{16}$$

Where:

$$\begin{aligned}\cos\theta = {} & sen\delta \cdot sen\varphi \cdot \cos\beta - sen\delta \cdot \cos\varphi \cdot sen\beta \cdot \cos\gamma + \\ & \cos\delta \cdot \cos\varphi \cdot \cos\beta \cdot \cos\gamma + \cos\delta \cdot sen\varphi \cdot sen\beta \cdot \cos\gamma \cdot \cos\omega + \\ & \cos\delta \cdot sen\beta \cdot sen\gamma \cdot sen\omega\end{aligned} \tag{17}$$

Being,

$$\delta = 21.11 - 13.28, \beta = 45°, \omega = variable, \Phi = 40.4°, and\ \gamma = \omega \tag{18}$$

4. Testing Method

We carry out different tests to compute the solar collector efficiency. To do so, we use the primary and secondary circuits. We use the primary solar collector circuit to calculate the energy transfer from the collector to the heating tank and to measure temperatures and solar radiation. The secondary solar collector circuit removes heat from the tank to induce a cooling process at the primary solar collector circuit that evacuates heat from the primary solar collector circuit, thus reducing the inlet temperature to the correct value. We measure solar radiation, inlet and outlet temperatures at the primary and secondary solar collector circuit, ambient temperature, and water flow during operation. A data acquisition system registers data for later analysis. An ultrasound flow meter measures the water flow at the primary circuit. The precision of the measurement is less than

0.1 l/min. An optical flow meter measures the water flow at the secondary solar collector circuit. The accuracy of the measuring is less than 0.01 l/min.

We measure parameters every minute and average values for a time interval of 10 minutes. We use an SKYE solar radiometer for solar radiation data, and thermocouples type K for temperature measurements. The accuracy is ±1 W/m^2 for the solar radiometer and ±0.5 K for the K-thermocouple.

Tests have been done at different flow rates, 0.8 l/min, 1.6 l/min and 2.4 l/min, to verify the accuracy of the methodology within a range from 0 to 0.050 for the equivalent temperature parameter; this is the current range in which a flat plate solar collector moves down to a zero efficiency value [21].

To calculate the efficiency, we use equation 15. This expression converts into the following one for our case:

$$\eta = \frac{\overset{*}{m}c\Delta T}{\alpha(\tau\alpha)IA} + \eta_o = a(\Delta T/I) + \eta_o = aT_{eq} + \eta_o \tag{19}$$

With $\Delta T = T_s - T_i$. We consider that a spherical collector collects solar radiation from different angles, which affects the α and ($\tau\alpha$) parameters [20]. The term η_o reflects the efficiency of the solar collector at the thermal short circuit.

To establish the equivalent temperature, we have set up the inlet temperature at the primary circuit using a thermal control device to remove enough energy from the tank. The secondary solar collector circuit acts as a thermal sink to maintain constant the inlet temperature at the primary solar collector circuit for the time needed. Outlet temperature will change according to the incoming solar radiation and collector efficiency. Because the flow is constant through the water pump, and α and ($\tau\alpha$) parameters are constant too if the time interval is not long, the parameter *a* remains constant; therefore, if we measure the solar radiation and the outlet temperature, we have the efficiency value. This procedure allows having a set of measures to obtain the efficiency draw. Suppose we change the heat removal rate; the inlet changes, so the equivalent temperature does. Repeating the former procedure for different values of heat removal produces a set of draws that we compare to validate the method.

5. Experimental Data and Analysis of Results (I)

To avoid unnecessary data, we have represented only a graph of the solar collector efficiency that indicates the global results for the different tests carried out during our testing; Figure 3 shows the so obtained values.

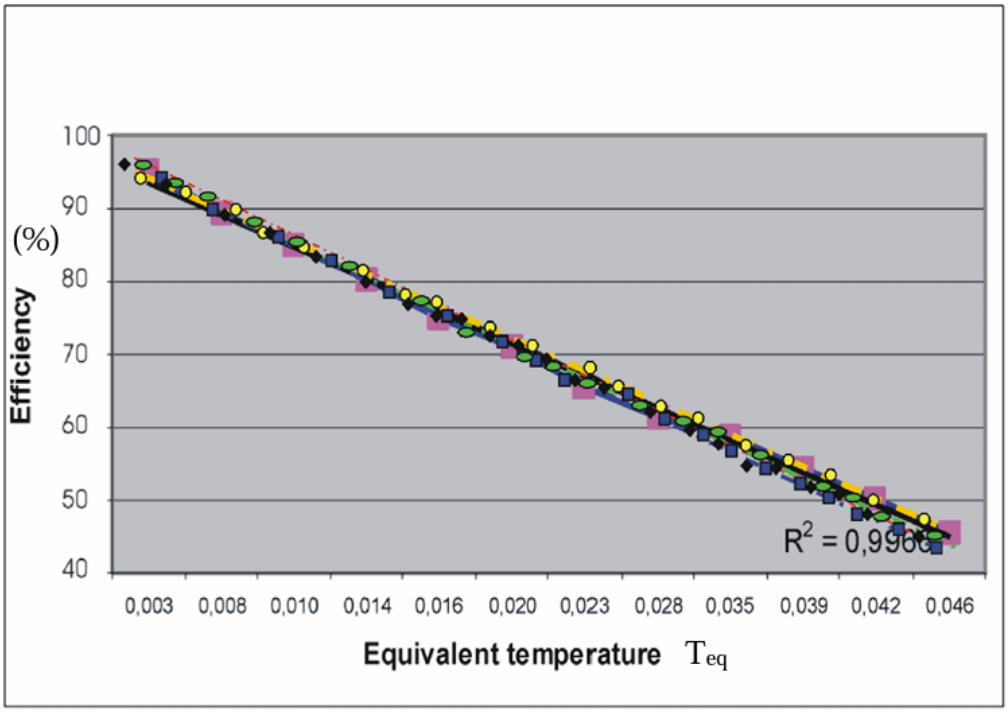

Figure 3 Evolution of the efficiency of the spherical solar collector with the equivalent temperature.

The equivalent temperature is defined as:

$$T_{eq} = \frac{T_{in} - T_{amb}}{I} \tag{20}$$

Where T_{in} and T_{amb} account for the inlet and ambient temperature, and I is the instantaneous solar radiation.

Spots of different colors correspond to the various types of the test; every color corresponds to a value of the inlet temperature and rate of heat removal; the correlation of all draws to a single one gives an RMS value of 0.9966 (see Figure 3) that validates the method within an error less than 0.4%.

We observe that the maximum efficiency corresponds to a value of 97%, which is an excellent result for the solar thermal collector compared to the average efficiency value at the thermal short circuit, which is about 85%.

Efficiency is even better at high equivalent temperature because the efficiency of a flat solar collector turns to zero at T_{eq} = 0.050; in our case the efficiency remains above 40% for the same equivalent temperature, which represents a considerable improvement of the solar performance response, especially at the high range where thermal solar collectors use to operate when solar radiation is high, and the energy demand is low.

If we compare both draws (see Figure 4), we can notice that the slope of the spherical collector is lower than that of the flat plate, which means the performance improves; on the other hand, from the linear regression, we obtain that the equation representing the efficiency evolution of the spherical collector is $\eta_{sph} = 97 - 1180T_{eq}$.

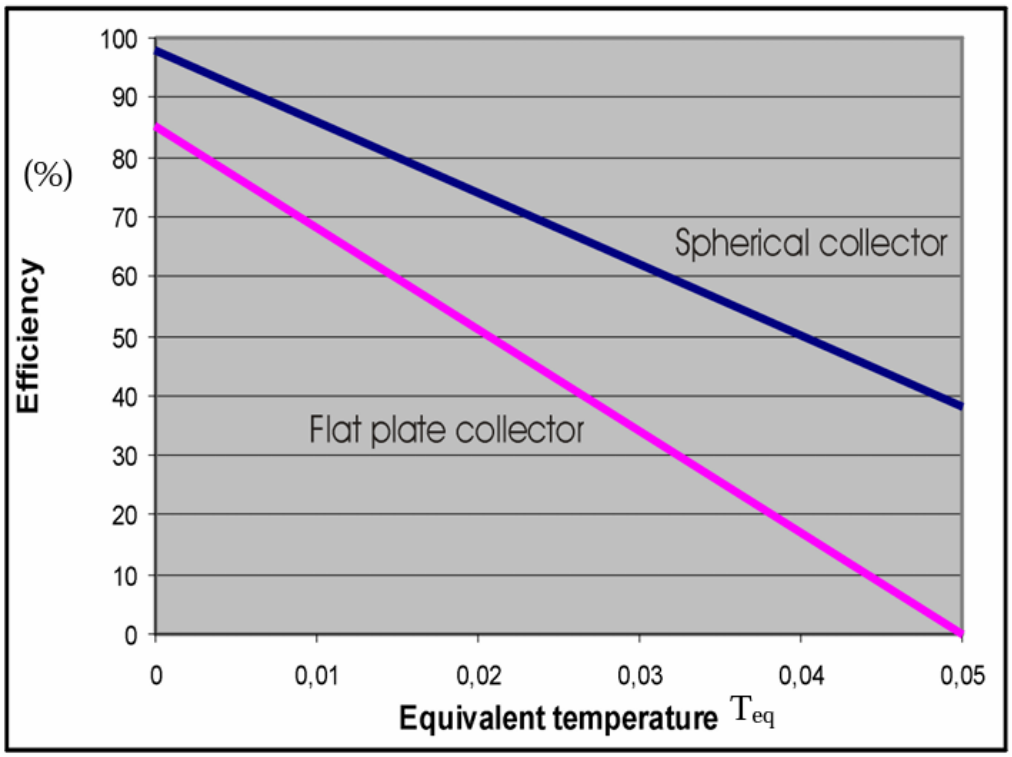

Figure 4 Comparison of the evolution of the efficiency for a spherical and flat plate solar collector with the equivalent temperature.

Extending the range up to the point where efficiency becomes zero, we obtain: $0 = 97 - 1180T_{eq} \rightarrow T_{eq} = 0.082$ Extending the range up to the point where efficiency becomes zero, we obtain: what means the spherical collector can operate for conditions where the flat plate does not say higher inlet temperatures for the same solar radiation; this is important because the inlet temperature matches the average tank temperature. If the collector can operate at a higher inlet temperature, the heating tank can increase its operating temperature on its way; therefore, the service water temperature from the secondary circuit will also be higher, increasing the operational time or being useful for an additional type of application.

6. Efficiency of the Compact System

Once we determine the solar collector efficiency, we analyze the performance of the compact solar system, the spherical collector unit and the storage tank.

The procedure for the characterization of the efficiency of the solar collector reproduces the method described before, now checking temperatures and water flow at the secondary circuit. According to the expression for the efficiency used before (eq. 19), the efficiency of the compact solar system can be expressed as:

$$\eta = \frac{\overset{*}{m}_{sc} c \Delta T_{\text{sec}}}{\alpha(\tau\alpha) I A} + \eta'_o = b(\Delta T_{\text{sec}}/I) + \eta'_o = bT'_{eq} + \eta'_o \qquad (21)$$

Temperatures and water flow are related to the second solar collector circuit.

7. Experimental Data and Analysis of Results (II)

Figure 5 shows the results for this new group of tests. We can observe that efficiency still is good, around 88% at a null value of T_{eq}, and above 30% at the high equivalent temperature range (T_{eq} = 0.050) (see Figure 5).

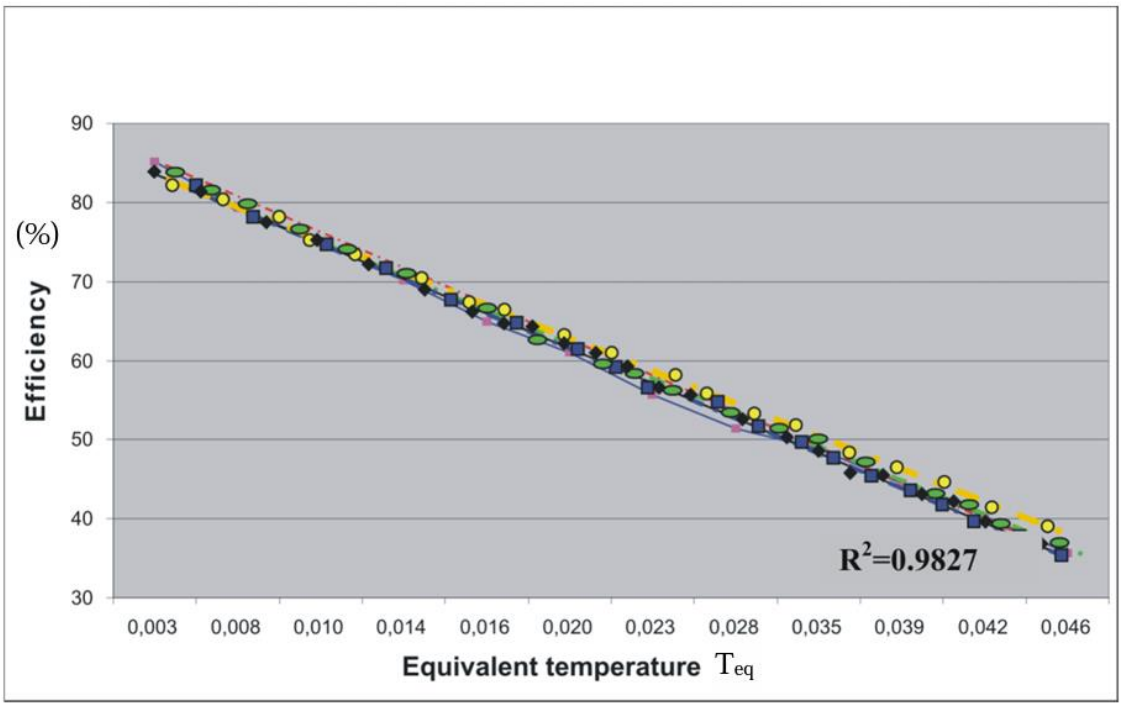

Figure 5 Evolution of the efficiency of a compact spherical solar system with the equivalent temperature.

Once again, every spot color corresponds to every type of test. We can see that the linear regression is very high, above 98%, which indicates that the methodology is accurate and the results are valid.

If we compare the efficiency curve with that obtained for a compact flat plate solar collector with the same characteristics, we realize that spherical collector performance still is better. The following graph (Figure 6) shows the comparative results for the spherical and flat plate solar collector of similar characteristics.

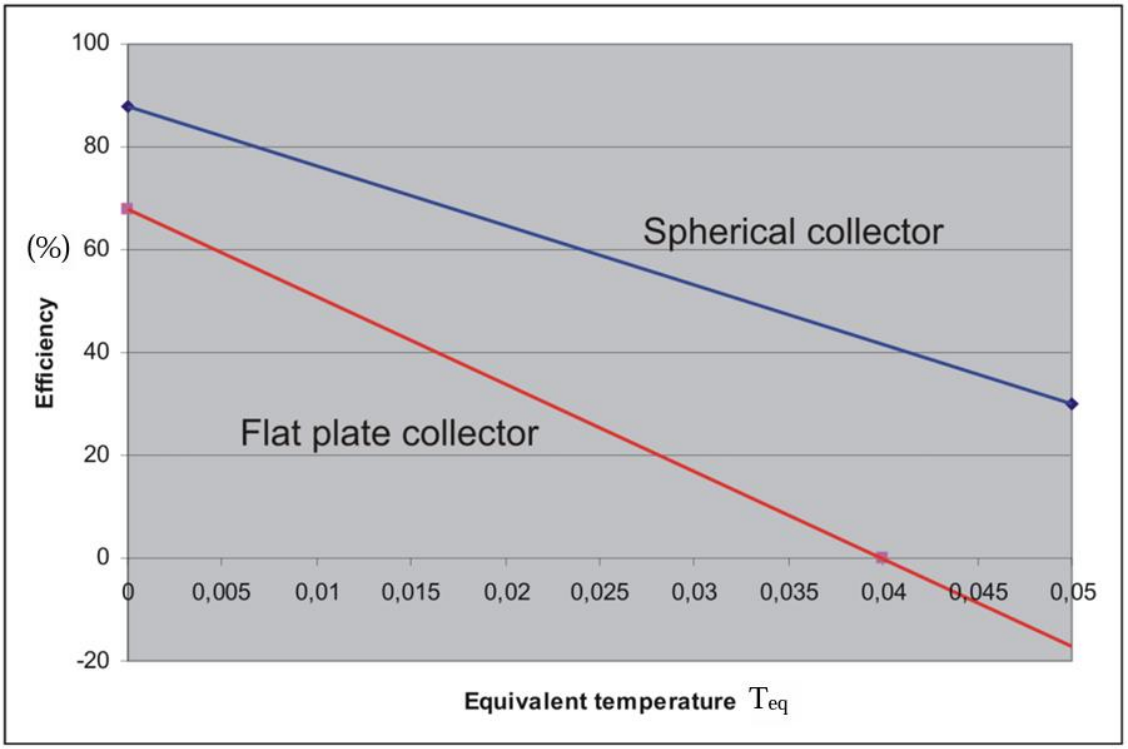

Figure 6 Comparative study of the evolution of the efficiency of compact systems, spherical and flat plate solar collector, with the equivalent temperature.

In this case, the compact spherical system shows an efficiency improvement at the thermal short circuit of 20% and about 40% at the zero efficiency point for the flat plate collector. For a compact spherical system, the equivalent temperature before the efficiency becomes zero is extended to 0.076, almost double the corresponding value of the flat plate system; this is because the collector structure covers the storage tank playing the role of an insulation cover, reducing thermal losses, thus increasing the outlet temperature and global efficiency.

8. Global Losses Coefficient

Collector thermal losses are mainly due to radiation phenomena from the absorber surface to the environment. This hypothesis bases on the fact that the convection between the surface and plastic cover is negligible, and the heat conduction is very low due to the low conductivity value of the air contained in the chamber between the surface and the outer cover. These losses are ruled by the Stefan-Boltzmann equation, where the external temperature is, in this case, the plastic cover temperature, as the absorber surface radiates to it instead of to the environment. Because the infrared transmission coefficient of the plastic cover is low, t_{IR} <0.15, we may consider that most of the radiation from the absorber surface is intercepted by the outer cover, thus being the radiation sink.

The following expression allows us to determine the global losses coefficient [22]:

$$U_L = (1/R_1 + R_2 + R_3) \tag{22}$$

Being;

$$1/R_1 = k/e_{fondo} \tag{23}$$

$$1/R_2 = h_r \tag{24}$$

$$h_r = \sigma \frac{(T_p + T_c)(T_p^2 + T_c^2)}{1/\varepsilon_p + 1/\varepsilon_c - 1} \tag{25}$$

$$1/R_3 = h_v + h_r' \tag{26}$$

$$h_r' = \varepsilon\sigma(T_p + T_s)(T_p^2 + T_s^2)\frac{(T_p - T_s)}{(T_p - T_a)} \tag{27}$$

$$h_v = 5.7 + 3.8v \tag{28}$$

The emissivity of the collector's surface can be determined using a method proposed by one of the authors [23].

9. Experimental Data and Analysis of Results (III)

Plate and cover temperatures have been monitored and registered during operation to compute the emissivity of the collector's surface. From a well-characterized surface, from the radiative heating point of view, the technique proposed by the author [24] allows for monitoring the sky temperature. We monitor the wind speed using a precision anemometer COMPUFLOW ALNOR GGA-65P. We use a data acquisition system to register all measured data. We compare the results obtained from this to those from the expression of the thermal balance of the solar collector:

$$U_L = \frac{I - (\dot{Q}/A_c F_R)}{T_i - T_a} \tag{29}$$

To validate the above hypothesis of thermal losses only due to radiation.

Using experimental data, the U_L value results:

$$\begin{aligned} U_L &= 4.3 W/m^2K \\ U_L &= 4.5 W/m^2K \end{aligned} \tag{30}$$

The result validates the hypothesis since the difference between the two values is less than 5%. Therefore, we accept the average value of the global thermal losses coefficient.

The so obtained value is considerably lower than the one for the flat plate collector under similar operational conditions, which is a typical value for flat plate collectors, meaning a reduction of more than 50% in the global thermal losses, mainly due to the covering effect the spherical structure has.

We can also obtain the global thermal losses coefficient from the slope of the curve in Figure 6; by doing so, we get a value of U_L = 4.438 W/m^2 for the spherical solar collector, very close to the results obtained in Equation 30.

For the flat-plate collector, the result is U_L = 6.542 W/m^2, representing an increase of 47.4% concerning the spherical solar collector, in close agreement with the reduction of 50% mentioned before.

The U_L value obtained for the spherical collector is the average of a group of values, so the thermal losses coefficient is not constant throughout the day interval. Because of the thermal evolution of the sphere, temperatures vary along the day, thus producing changes in the UL value. This value is maximum at midday, with a dome in the values during the central hours of the day, and minimum at sunrise and sunset. The following graph shows the variation of the UL value as indicated (Figure 7).

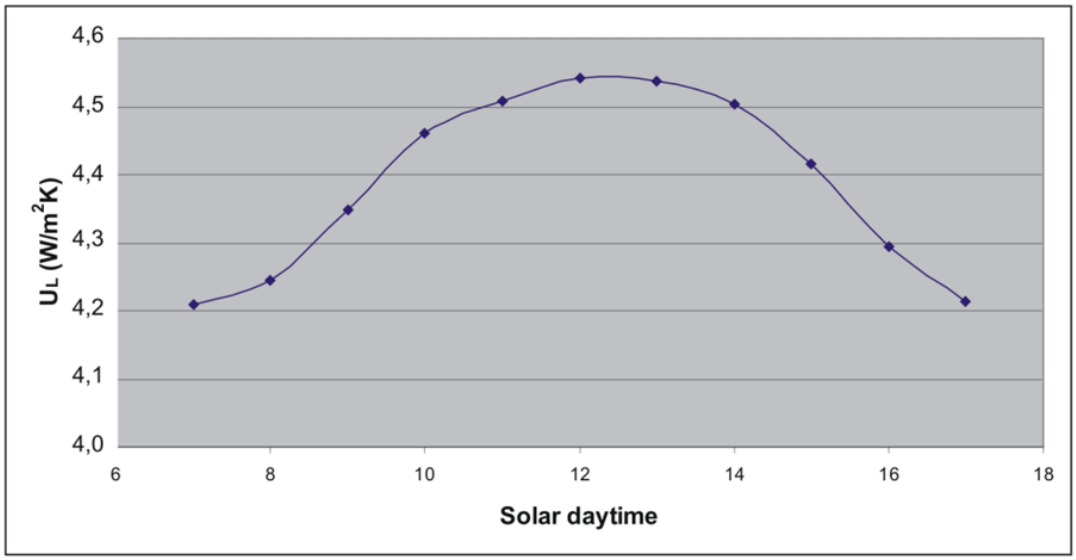

Figure 7 Evolution of the global losses coefficient for a spherical collector with the solar daytime.

The variation of the U_L coefficient indicates that the thermal evolution of the prototype influences thermal losses. This variation approximately follows solar radiation change during the day, which means that the collector's performance will benefit from this behavior, the maximum radiation the maximum UL, and vice versa.

10. Advantages and Drawbacks

Among the advantages of spherical solar collectors, we can mention higher energy efficiency and lower global thermal losses coefficient, which result in increased performance. Additionally, the spherical solar collector structure provides better protection for the storage tank against thermal losses since the current configuration (compact design) manufactures a built-in thermal tank; therefore, the spherical surface acts as a protective case for the storage tank.

On the contrary, the spherical solar collector engineering design is more complex and costly and requires a more resistant support structure to stand for the increased weight of the assembly. Another drawback is the higher thermal losses at night because of the larger radiative surface, especially in cold climates.

Nevertheless, the sum of the advantages compensates for the drawbacks, making the spherical geometry a suitable solution to improve the performance of low-temperature solar thermal collectors.

11. Conclusions

The study and characterization of the spherical solar collector lead us to the following conclusions:

- The spherical shape collects more energy than flat plate collectors without the need for a solar tracking system.
- Spherical collector performance is better because of the collection of additional radiation.
- Global efficiency increases at all ranges of equivalent temperature. The increase varies from 13% to 38% for low and high Teq, respectively.
- Spherical collector enlarges time of operation due to the fact the equivalent temperature is higher for zero efficiency; also, it can operate in a region where a flat plate collector does not produce positive energy gain.
- A spherical shape can be adequate for some applications that require longer thermal discharges.
- The spherical collector structure produces additional benefits because of the protective action of the storage tank. This protection reduces thermal losses, improves compact system performance, and increases global efficiency.
- The increase in global efficiency when using the compact structure of a combined solar collector and tank is 15% at the low range of equivalent temperature, and 40% at the thigh range.
- The global losses coefficient of a spherical collector is much lower, 50%, than that of a flat plate having equivalent characteristics.

Nomenclature

A_c	Collector aperture area
C_b	Conductance
C_p	Specific heat coefficient
D	Diameter of the duct
e	Thickness
F	Plate to duct heat transfer coefficient
F_R	Heat transfer coefficient
h	Heat transfer coefficient due to conduction or convection
h_{f_i}	Duct to fluid heat transfer coefficient
I	Solar irradiance
I_c	Solar radiation threshold
I_{ON}	Normal solar radiation to collector's surface
k	Thermal conductivity
m	Thermal resistance coefficient
$\dot{m}$	Mass flow
$\dot{Q}$	Heat or energy
$\dot{Q}_L$	Thermal losses flow
Q_u	Heat or energy gain
R	Thermal resistance
r_{Q_L}	Ratio of thermal losses

S	Surface or area
T_a	Ambient temperature
T_{cv}	Cover temperature
T_e	Temperature of the thermal sink
T_{eq}	Equivalent temperature
T_i	Inlet temperature
T_p	Plate temperature
T_s	Outlet temperature
ΔT_{sec}	Temperature gap at the secondary circuit
U_L	Thermal losses coefficient
U_{L_c}	Thermal losses coefficient due to conductive effects
U_{L_t}	Thermal losses coefficient due to transmission effects
W	Space interval between ducts
α	Absorption coefficient
β	Tilt
δ	Declination
ε	Emissivity
ϕ	Latitude
φ	Utilizability
γ	Azimuth
η	Collector's efficiency
θ_z	Azimuthal incidence angle
θ	Incidence angle
σ	Stefan-Boltzmann coefficient
τ	Transmission coefficient
ω	Hourly angle
$\dot{\xi}$	Emitted energy

Author Contributions

The author did all the research work of this study.

Competing Interests

The author has declared that no competing interests exist.

References

1. Armenta-Déu C, Lukac B, Incidence angle modifier. Its incidence on solar collector utilizability and on energy received. Solar Radiation Data, Project EUFRAT. Solar Energy Research and Development in the European Community; 1990; FD/07.
2. Scharmer K. Towards a new atlas of solar radiation in Europe. Int J Sol Energy. 1994; 15: 81-87.
3. Bourges B. Climatic data handbook for Europe. Philip Drive, Norwell, MA, USA: Kluwer Academic Publishers; 1992. p. 295.

4. Maia CB, Ferreira AG, Hanriot SM. Evaluation of a tracking flat-plate solar collector in Brazil. Appl Therm Eng. 2014; 73: 953-962.
5. Notton G, Diaf S. Available solar energy for flat-plate solar collectors mounted on a fixed or tracking structure. Int J Green Energy. 2016; 13: 181-190.
6. Gordon JM, Kreider JF, Reeves P. Tracking and stationary flat plate solar collectors: Yearly collectible energy correlations for photovoltaic applications. Sol Energy. 1991; 47: 245-252.
7. Bakır Ö. Experimental investigation of a spherical solar collector. Doctoral Thesis, Ankara, Turkey: Middle East Technical University; 2006.
8. Samanta B, Al Balushi KR. Estimation of incident radiation on a novel spherical solar collector. Renew Energ. 1998; 14: 241-247.
9. Yadav AS, Gattani A. Solar thermal air heater for sustainable development. Mater Today. 2022; 60: 80-86.
10. Yadav AS, Shukla OP, Bhadoria RS. Recent advances in modeling and simulation techniques used in analysis of solar air heater having ribs. Mater Today. 2022; 62: 1375-1382.
11. Yadav AS, Agrawal A, Sharma A, Sharma S, Maithani R, Kumar A. Augmented artificially roughened solar air heaters. Mater Today. 2022; 63: 226-239.
12. Mahdi K, Bellel N. Development of a spherical solar collector with a cylindrical receiver. Energy Procedia. 2014; 52: 438-448.
13. Gaspar F, Deac T, Tutunaru LV, Moldovanu D. Experimental study on the sun tracking ability of a spherical solar collector. Energy Procedia. 2016; 85: 220-227.
14. Gaspar F, Balan M, Jantchi L, Ros V. Evaluation of global solar radiation received by a spherical solar collector. Bull UASVM Agric. 2012; 69: 128-135.
15. Elhefnawy MA, Ahmed AR, Awad MM. Experimental investigation on the performance of spherical solar collector for water heating. Mansoura Eng J. 2020; 41: 27-37.
16. Carvalho MJ, Collares-Pereira M. Correlations for the utilizability function. Solar Radiation Data, Project EUFRAT. Solar Energy Research and Development in the European Community; 1990; FD/04.
17. Armenta-Déu C. Estudio de sistemas compactos para producción de ACS. Internal Report GER-UCM. Madrid: Complutense University of Madrid; 1994.
18. Hernando J. Análisis de pérdidas térmicas en captadores solares, informe final Diplomatura Estudios Avanzados (DEA). Final Report. Madrid: Universidad Complutense; 2004.
19. Duffie JA, Beckman WA, Blair N. Solar engineering of thermal processes, photovoltaics and wind. Hoboken, New Jersey, USA: John Wiley & Sons; 2020.
20. Armenta-Deu C, Lukac B. A correlation model to compute the incidence angle modifier and to estimate its effect on collectible solar radiation. Renew Energ. 1991; 1: 803-809.
21. SPHERASOL. INTERECO S.n.c. Colector-depósito esférico SferaSol [Internet]. Available from: https://www.youtube.com/watch?v=Zwro1bQotnU.
22. SOLAHART. Technical data. Flat plate solar collector. Available from: https://www.solahartespaña.com.
23. Santos I. Estudio y caracterización de un captador de simetría esférica para producción de ACS por energía solar. Master Thesis. Faculty of Physics, Complutense University of Madrid, 2006.
24. Armenta-Déu C, Donaire T, Hernando J. Thermal analysis of a prototype to determine radiative cooling thermal balance. Renew Energ. 2003; 28: 1105-1120.